GEOPHYSICAL RESEARCH LETTERS, VOL. 20, NO. 15, PAGES 1643-1646, AUGUST 6, 1993

MONITORING OF STRAIN RELEASE IN CENTRAL AND NORTHERN CALIFORNIA USING BROADBAND DATA

Barbara Romanowicz, Douglas Dreger, Michael Pasyanos and Robert Uhrhammer

Seismographic Station, University of California at Berkeley, Berkeley, CA, 94720

Abstract. Systematic cataloguing of seismic moment, depth and mechanism of regional earthquakes down to magnitude M~4 can now be achieved in close to real-time using data from sparse networks of digital broadband stations. The procedure we have developed relies on 3 independent methods for the determination of moment tensor, providing confidence limits on the results. We show the results of application to the seismicity in central and northern California for a one year period starting in March 1992 and illustrate how patterns of stress and strain release can now be monitored systematically and reliably in a timely fashion.

Introduction

The mode of monitoring of seismic activity in seismically active areas is undergoing a quantum jump owing to the concurrence of two factors: the deployment of digitally telemetered broadband networks and progress in waveform and spectral techniques for source parameter retrieval. In California, with the development of the TERRAscope network in the South (Kanamori and Hauksson, 1991) and the Berkeley Digital Seismic Network (BDSN) in the North (Bolt et al., 1988; Romanowicz et al., 1992), the traditional determination of location and local magnitude can now be complemented by systematic and robust estimation of seismic moment and mechanism as well as other rupture parameters, this for a wide range of earthquake sizes and in a close to real-time fashion. In the case of the BDSN, the data are transmitted continuously to a central location at U.C. Berkeley, making it possible, in principle, to obtain solutions within several minutes after the occurrence of the earthquake, provided some automation is implemented (Ekstrom, 1992).

The ability to systematically compile source parameters for moderate and large earthquakes (magnitude M>4), within a short time after their occurrence, extends the concept of the CMT catalog (Dziewonski et al., 1988) available for "global" earthquakes of M> ~5.5. Such regional catalogs increase the scientific potential of seismicity studies, by providing the means to better characterize the regional strain release in space and time. When these parameters are estimated in close to real-time, they also provide critical information for the assessment of areas of potential damage and for the forecasting of the rate of aftershock occurrence in the case of a large earthquake.

At UC Berkeley, we are taking a three-tiered approach to systematically determine moment tensors of central and northern California earthquakes in close to real-time, using a combination of surface waves in the spectral domain, body waveforms and near-field waveform data. We here briefly describe and illustrate these three techniques and present the results of application to earthquakes in the past year.

Methods of analysis

Surface wave moment tensor inversion

Surface wave moment tensor inversion has been shown to be effective at the global scale (e.g. Patton, 1980; Kanamori and Given, 1981) and regional scale (Thio and Kanamori, 1991). We have adapted to the scale of California, a two-step moment tensor inversion originally developed for teleseismic surface waves at intermediate periods (Romanowicz, 1982) and later extended to the case of global mantle waves (e.g. Romanowicz and Monfret, 1986). This technique has previously been applied at the sub-continental scale for moderate size earthquakes in the western U.S. (Patton and Zandt, 1991). For the regional case considered here, we limit ourselves to Love and Rayleigh waves in the period range 15-50 sec, which allows the study of frequent moderate size earthquakes (M_L~ 3-5). Distances are typically in the range 100-500 km, and data from stations at shorter distances are not used to avoid contamination by Pnl waves.

The two-step moment tensor inversion takes advantage of the simple theoretical form of the source azimuthal radiation pattern by, in the first step, using Fourier analysis in azimuth, to eliminate poorly modeled short wavelength path effects. In the second step, the azimuthal coefficients are inverted at a series of trial depths to obtain estimates of centroid depth and moment tensor (see Romanowicz and Monfret, 1986 for a detailed presentation). The advantage of this method over more conventional "one-step" inversions is that a laterally homegeneous approximate model for propagation corrections is generally sufficient for accurate estimation of the moment tensor. However, for the Fourier analysis to be valid, some azimuthal sampling around the source is necessary.

Body waveform modelling

The body waveform modelling technique is described in Dreger and Helmberger (1993) and requires fewer stations than the surface wave method. In regions where the propagation paths are well calibrated a single, three-component station is sufficient. This method utilizes three component body waveforms recorded at local (less than 100 km) and regional (100 to 1000 km) distances to determine the seismic moment tensor. Green's functions are computed initially for models used to routinely locate earthquakes. Source depth is determined by iteratively inverting the data with Green's functions obtained for different source depths and choosing the solution that minimizes the residual. The models are finetuned by forward modelling of the broadband displacement waveforms. In southern California, Dreger and Helmberger (1993) found that a simple one-dimensional crustal model was adequate to explain many details of the broadband waveforms recorded by the TERRAscope network. In central and northern California, several models are currently being tested. This approach is more labor intensive at present than the surface wave inversion, but through the process of calibrating paths to explain body wave propagation a catalog of Green's functions is being compiled for systematic use in future analysis.

Near Field Moment Tensor Inversion

The third approach has the advantage of being simple, of requiring data at a single station, and of allowing retrieval of moment tensors for earthquakes down to magnitudes less than 2, provided they are located at close range to one of the broadband stations (Uhrhammer, 1992). This is particularly useful for monitoring the seismic activity along the Bay Area

Copyright 1993 by the American Geophysical Union.

Paper Number 93GL01540
0094-8534/93/93GL-01540$03.00

faults (San Andreas, Hayward Fault, Calaveras fault) as well as on the San Andreas Fault in the vicinity of Parkfield. A half-space model is used and the information is essentially provided by the near-field ramps between the P and S waves. The feasibility of using near field data was demonstrated by Kanamori et al. (1990) and the details of the method are described elsewhere (Uhrhammer, in preparation).

Application to Central and Northern California

For the past year, we have been systematically estimating moment tensor and depth of earthquakes in central and northern California using a combination of the three methods described above. Table I lists the results obtained for all events of M> 3.5 for which a stable solution was obtained, and is complete down to M 4.5, with the exclusion of the Cape Mendocino sequence of April 1992. These large earthquakes and some of their aftershocks have been studied elsewhere. Results for several events in adjacent regions are also given. From Table I, we see that, when several solutions are available for an event, the mechanisms agree to within 10°, regardless of type, while estimates of moment-magnitude differ by at most 0.3 units of magnitude. By careful path calibration, we hope to reduce this scatter down to 0.1 unit in the future. The present estimates are however more consistent with each other than with the estimate of local magnitude (M_L), which does not rigourously account for source radiation pattern nor frequency content. They are also consistent with results from other studies, when available (e.g. Thio et al., 1991).

Figure 1a shows the mechanisms of the events listed in Table I, representing approximately one year of moment release for central and northern California and adjacent regions, excluding the Cape Mendocino sequence and the southern California sequences related to the Joshua Tree and Landers earthquakes. Figure 1b shows examples of solutions obtained using the near-field inversion procedure, along the Calaveras fault.

Figure 1 reflects the predominantly strike-slip character of the tectonic strain release along the central and northern California portion of the Pacific/North American plate boundary. Earthquakes located directly on the San Andreas fault (Parkfield: 10/20/92, 04/04/92) or its principal splays (Hayward Fault, 01/15/93; Calaveras fault: Gilroy 01/16/93 and figure 1b) indicate a direction of maximum compressive stress rotated ~45° from the strike of the fault, while earthquakes not directly on these faults show mechanisms that

TABLE 1. Source parameters as obtained in this study. Epicentral coordinates are from the Berkeley catalog (determined using short period data). Asterix indicates the solution plotted in FIgure 1. Key to methods: (1) Regional surface wave inversion, (2) Regional body waveform inversion (3) Single station near-field inversion.

Location	Date	O.T. (UTC)	Lat. (°N)	Lon. (°W)	Depth (km)	M_L	M_w	M_o (N-m)	Str/Dip/Rake	Method
Mendocino	030892	03:43	40.23	124.29	12	5.2	5.2	$6.8 * 10^{16}$	102/74/145	(1)*
Mendocino	050592	10:46	40.32	124.36	12	4.5	4.4	$4.1 * 10^{15}$	89/74/-162	(1)*
Mendocino	060592	21:46	40.29	124.55	10	4.8	4.9	$2.9 * 10^{16}$	133/63/-89	(1)*
Skull Mt.	062992	10:14	36.66	116.23	8	6.2	5.6	$3.5 * 10^{17}$	43/66/-73	(1)*
					8		5.6	$2.6 * 10^{17}$	34/44/-70	(2)
Fallon, NV	072092	07:20	39.34	119.11	8	4.5	4.5	$7.2 * 10^{15}$	328/86/-141	(1)
					11		4.4	$4.0 * 10^{15}$	334/66/-161	(2)*
SW Utah	090292	10:26	37.05	113.46	20	5.8	5.6	$3.2 * 10^{17}$	10/48/-90	(1)*
					11		5.3	$9.7 * 10^{16}$	7/47/-91	(2)
Coalinga	091692	06:14	35.97	119.87	8	4.3	4.1	$1.4 * 10^{15}$	310/48/111	(1)*
Geysers	091992	23:04	38.86	122.79	4	4.9	4.8	$1.7 * 10^{16}$	175/85/172	(1)*
					2		4.5	$6.0 * 10^{15}$	2/85/162	(2)
Parkfield	102092	05:28	35.92	120.49	10	4.3	4.6	$9.6 * 10^{15}$	234/89/353	(1)*
Mono Basin	101092	17:54	37.99	118.58	6	4.1	3.9	$9.7 * 10^{14}$	167/75/160	(1)*
					7		3.8	$5.3 * 10^{14}$	345/75/-172	(2)
Big Bear	112792	16:00	34.34	116.89	7	5.6	5.4	$1.2 * 10^{17}$	223/82/20	(1)*
					5		5.3	$8.5 * 10^{16}$	215/70/35	(2)
Big Bear	120492	02:08	34.33	116.95	6	5.4	5.3	$9.2 * 10^{16}$	283/46/106	(1)*
					5		5.0	$3.8 * 10^{16}$	249/66/54	(2)
Quincy	122592	04:25	39.95	120.84	14	4.2	3.8	$5.8 * 10^{14}$	205/80/-2	(1)*
					14		3.7	$4.5 * 10^{14}$	213/80/22	(2)
					23		3.7	$4.2 * 10^{14}$	230/83/-7	(3)
Mono Basin	011193	13:32	38.02	118.74	6	4.0	3.9	$9.1 * 10^{14}$	179/83/172	(1)*
Mono Basin	011193	18:19	38.05	118.73	8	3.9	3.9	$8.2 * 10^{14}$	168/83/163	(1)*
					11		3.8	$5.5 * 10^{14}$	175/50/165	(2)
Kensington	011593	11:13	37.92	122.29	6	3.2	3.4	$1.6 * 10^{14}$	118/77/-170	(1)
					5		3.1	$5.0 * 10^{13}$	323/66/-167	(2)
					7		3.2	$7.2 * 10^{13}$	311/82/-175	(3)*
Gilroy	011693	06:29	37.03	121.46	8	5.3	5.1	$4.5 * 10^{16}$	144/86/-179	(1)*
					7		4.9	$2.4 * 10^{16}$	331/83/166	(2)
					8		5.0	$4.0 * 10^{16}$	336/82/140	(3)
Geysers	011893	23:27	38.85	122.78	6	3.9	4.1	$1.6 * 10^{15}$	4/42/-93	(1)*
					4		4.1	$1.3 * 10^{15}$	5/30/-58	(2)
Geysers	011993	00:24	38.84	122.78	6	3.8	3.9	$8.2 * 10^{14}$	2/51/-102	(1)*
					4		3.9	$7.5 * 10^{14}$	-5/28/-58	(2)
Pyramid Lake, NV	021093	21:48	40.40	119.58	12	5.1	4.5	$6.0 * 10^{15}$	3/55/-108	(1)*
					11		4.6	$9.0 * 10^{15}$	0/51/-113	(2)
Parkfield	040493	05:21	35.95	120.51	8	4.3	4.4	$4.5 * 10^{15}$	143/85/177	(1)*
					7		4.2	$2.3 * 10^{15}$	146/84/-175	(2)
					6		4.4	$3.9 * 10^{15}$	312/82/177	(3)
Cataract Creek	042593	09:29	35.60	112.10	8	4.6	4.9	$2.5 * 10^{16}$	96/49/-97	(1)*
					11		4.6	$1.0 * 10^{16}$	298/53/-64	(2)
Cataract Creek	042993	08:21	35.60	112.10	8	5.7	5.4	$1.6 * 10^{17}$	105/48/-94	(1)*
					11		5.2	$6.1 * 10^{16}$	306/48/-65	(2)

faults (San Andreas, Hayward Fault, Calaveras fault) as well as on the San Andreas Fault in the vicinity of Parkfield. A half-space model is used and the information is essentially provided by the near-field ramps between the P and S waves. The feasibility of using near field data was demonstrated by Kanamori et al. (1990) and the details of the method are described elsewhere (Uhrhammer, in preparation).

Application to Central and Northern California

For the past year, we have been systematically estimating moment tensor and depth of earthquakes in central and northern California using a combination of the three methods described above. Table I lists the results obtained for all events of M> 3.5 for which a stable solution was obtained, and is complete down to M 4.5, with the exclusion of the Cape Mendocino sequence of April 1992. These large earthquakes and some of their aftershocks have been studied elsewhere. Results for several events in adjacent regions are also given. From Table I, we see that, when several solutions are available for an event, the mechanisms agree to within 10°, regardless of type, while estimates of moment-magnitude differ by at most 0.3 units of magnitude. By careful path calibration, we hope to reduce this scatter down to 0.1 unit in the future. The present estimates are however more consistent with each other than with the estimate of local magnitude (M_L), which does not rigourously account for source radiation pattern nor frequency content. They are also consistent with results from other studies, when available (e.g. Thio et al., 1991).

Figure 1a shows the mechanisms of the events listed in Table I, representing approximately one year of moment release for central and northern California and adjacent regions, excluding the Cape Mendocino sequence and the southern California sequences related to the Joshua Tree and Landers earthquakes. Figure 1b shows examples of solutions obtained using the near-field inversion procedure, along the Calaveras fault.

Figure 1 reflects the predominantly strike-slip character of the tectonic strain release along the central and northern California portion of the Pacific/North American plate boundary. Earthquakes located directly on the San Andreas fault (Parkfield: 10/20/92, 04/04/92) or its principal splays (Hayward Fault, 01/15/93; Calaveras fault: Gilroy 01/16/93 and figure 1b) indicate a direction of maximum compressive stress rotated ~45° from the strike of the fault, while earthquakes not directly on these faults show mechanisms that

TABLE 1. Source parameters as obtained in this study. Epicentral coordinates are from the Berkeley catalog (determined using short period data). Asterix indicates the solution plotted in FIgure 1. Key to methods: (1) Regional surface wave inversion, (2) Regional body waveform inversion (3) Single station near-field inversion.

Location	Date	O.T. (UTC)	Lat. (°N)	Lon. (°W)	Depth (km)	M_L	M_w	M_o (N-m)	Str/Dip/Rake	Method
Mendocino	030892	03:43	40.23	124.29	12	5.2	5.2	$6.8*10^{16}$	102/74/145	(1)*
Mendocino	050592	10:46	40.32	124.36	12	4.5	4.4	$4.1*10^{15}$	89/74/-162	(1)*
Mendocino	060592	21:46	40.29	124.55	10	4.8	4.9	$2.9*10^{16}$	133/63/-89	(1)*
Skull Mt.	062992	10:14	36.66	116.23	8	6.2	5.6	$3.5*10^{17}$	43/66/-73	(1)*
					8		5.6	$2.6*10^{17}$	34/44/-70	(2)
Fallon, NV	072092	07:20	39.34	119.11	8	4.5	4.5	$7.2*10^{15}$	328/86/-141	(1)
					11		4.4	$4.0*10^{15}$	334/66/-161	(2)*
SW Utah	090292	10:26	37.05	113.46	20	5.8	5.6	$3.2*10^{17}$	10/48/-90	(1)*
					11		5.3	$9.7*10^{16}$	7/47/-91	(2)
Coalinga	091692	06:14	35.97	119.87	8	4.3	4.1	$1.4*10^{15}$	310/48/111	(1)*
Geysers	091992	23:04	38.86	122.79	4	4.9	4.8	$1.7*10^{16}$	175/85/172	(1)*
					2		4.5	$6.0*10^{15}$	2/85/162	(2)
Parkfield	102092	05:28	35.92	120.49	10	4.3	4.6	$9.6*10^{15}$	234/89/353	(1)*
Mono Basin	101092	17:54	37.99	118.58	6	4.1	3.9	$9.7*10^{14}$	167/75/160	(1)*
					7		3.8	$5.3*10^{14}$	345/75/-172	(2)
Big Bear	112792	16:00	34.34	116.89	7	5.6	5.4	$1.2*10^{17}$	223/82/20	(1)*
					5		5.3	$8.5*10^{16}$	215/70/35	(2)
Big Bear	120492	02:08	34.33	116.95	6	5.4	5.3	$9.2*10^{16}$	283/46/106	(1)*
					5		5.0	$3.8*10^{16}$	249/66/54	(2)
Quincy	122592	04:25	39.95	120.84	14	4.2	3.8	$5.8*10^{14}$	205/80/-2	(1)*
					14		3.7	$4.5*10^{14}$	213/80/22	(2)
					23		3.7	$4.2*10^{14}$	230/83/-7	(3)
Mono Basin	011193	13:32	38.02	118.74	6	4.0	3.9	$9.1*10^{14}$	179/83/172	(1)*
Mono Basin	011193	18:19	38.05	118.73	8	3.9	3.9	$8.2*10^{14}$	168/83/163	(1)*
					11		3.8	$5.5*10^{14}$	175/50/165	(2)
Kensington	011593	11:13	37.92	122.29	6	3.2	3.4	$1.6*10^{14}$	118/77/-170	(1)
					5		3.1	$5.0*10^{13}$	323/66/-167	(2)
					7		3.2	$7.2*10^{13}$	311/82/-175	(3)*
Gilroy	011693	06:29	37.03	121.46	8	5.3	5.1	$4.5*10^{16}$	144/86/-179	(1)*
					7		4.9	$2.4*10^{16}$	331/83/166	(2)
					8		5.0	$4.0*10^{16}$	336/82/140	(3)
Geysers	011893	23:27	38.85	122.78	6	3.9	4.1	$1.6*10^{15}$	4/42/-93	(1)*
					4		4.1	$1.3*10^{15}$	5/30/-58	(2)
Geysers	011993	00:24	38.84	122.78	6	3.8	3.9	$8.2*10^{14}$	2/51/-102	(1)*
					4		3.9	$7.5*10^{14}$	-5/28/-58	(2)
Pyramid Lake, NV	021093	21:48	40.40	119.58	12	5.1	4.5	$6.0*10^{15}$	3/55/-108	(1)*
					11		4.6	$9.0*10^{15}$	0/51/-113	(2)
Parkfield	040493	05:21	35.95	120.51	8	4.3	4.4	$4.5*10^{15}$	143/85/177	(1)*
					7		4.2	$2.3*10^{15}$	146/84/-175	(2)
					6		4.4	$3.9*10^{15}$	312/82/177	(3)
Cataract Creek	042593	09:29	35.60	112.10	8	4.6	4.9	$2.5*10^{16}$	96/49/-97	(1)*
					11		4.6	$1.0*10^{16}$	298/53/-64	(2)
Cataract Creek	042993	08:21	35.60	112.10	8	5.7	5.4	$1.6*10^{17}$	105/48/-94	(1)*
					11		5.2	$6.1*10^{16}$	306/48/-65	(2)

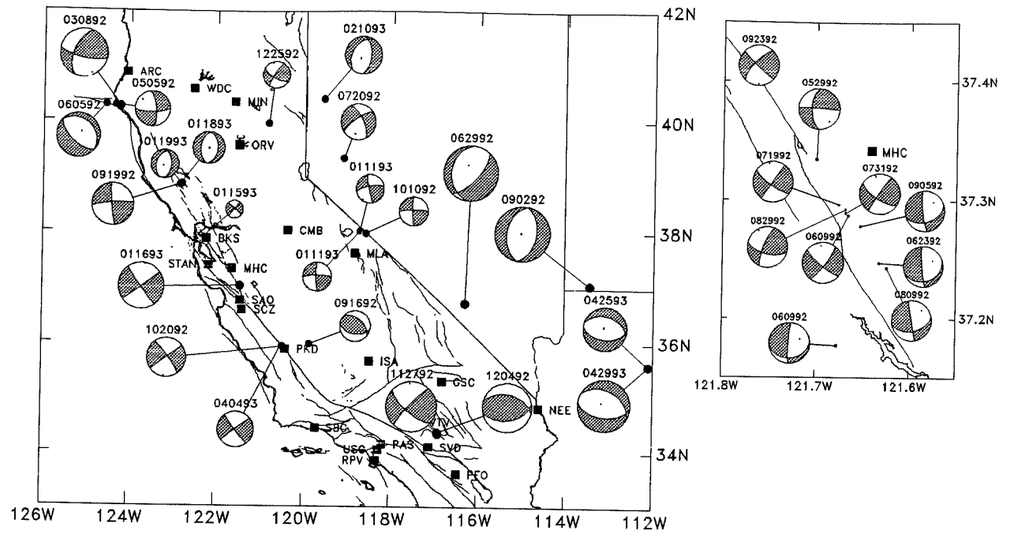

Fig. 1. a) Source mechanisms obtained for the events listed in Table I. These mechanisms represent the best double couple fits to the moment tensors obtained by surface wave inversion and are scaled to the value of the scalar moment. The locations of stations of the BDSN and TERRAscope networks are given (squares). b) Close-in view of the vicinity of station MHC (near Calaveras fault) showing some solutions obtained using near field data, for recent events of magnitude between 2 and 3.

are consistent with the regional stress pattern described by Zoback et al. (1987), with maximum compressive stresses normal to the strike of the San Andreas system in its vicinity (e.g. Figure 1b and 09/16/92 Coalinga, 09/19/92), rotating progressively towards the north in western California and Nevada (eg events east of longitude 121°W) as well as southern California (e.g. 11/27/92 and 12/04/92). The pattern changes from dominantly strike-slip to normal faulting in the Basin and Range province (e.g. Patton and Zandt, 1991). The mechanisms of the two April 1993 Cataract Creek events in Arizona are consistent with northeast-southwest extension in the Colorado Plateau (Zoback and Zoback, 1980). Also, in the Geysers region, stresses are likely controlled by the local geothermal field properties. The mechanisms obtained for the events in the vicinity of the Mendocino triple junction show a direction of maximum compressive stress oriented northwest-southeast, consistent with motion along the east west trending Mendocino Fault but not with the stress field of the main shock of the April 25, 1992 Mendocino sequence (Oppenheimer et al., 1993).

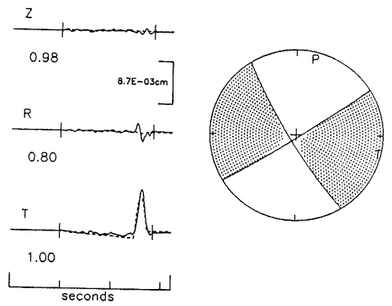

Fig. 2. Fit to the phase (top) and amplitude (bottom) data (circles) at a period of 25.6 sec obtained by surface wave inversion for the 01/16/93 Gilroy event (Mw~5.0).

The complementary use of 3 methods to obtain estimates of seismic moment and mechanism allows us to 1) evaluate the reliability of the mechanism and the accuracy of the moment estimate rapidly after the occurrence of the event, 2) obtain moment tensors for a wide range of sizes.To illustrate these points, we show in Figures 2 and 3 examples of respective fits

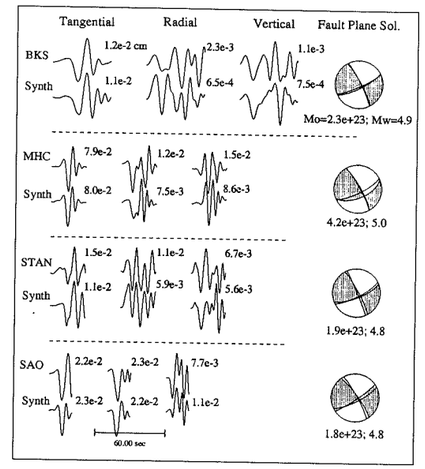

Fig. 3. Observed (top traces) low-pass filtered displacement body waveforms at stations of the BDSN for the Gilroy event of 01/16/93 compared to best fit synthetic seismograms (bottom traces). The synthetics were computed using an F-K integration procedure, a velocity model developed for the San Francisco Bay Area and the source parameters using single station bodywave inversion (shaded solution). The unshaded solution was obtained by simultaneous inversion of all the stations.

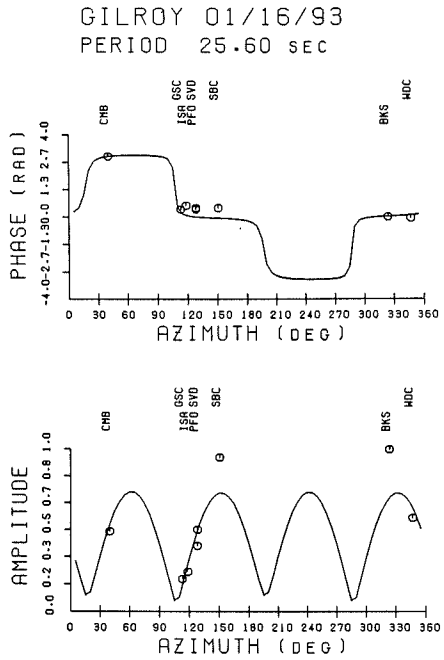

Fig. 4. Example of near-field moment tensor inversion for a small earthquake (Mw 2.9, 11/16/92) which occurred 4.8 km southwest of station MHC. The displacement waveforms (solid lines) are compared to best fitting synthetics (dashed lines). The number below each trace is the correlation coefficient between observed and synthetics. The south-east trending plane of the solution (strike 148, dip 87, rake -177) is within a few degrees of the general trend of the Calaveras Fault in the region.

to the surface wave and body wave data achieved for the Gilroy event of 01/16/93. The mechanisms obtained by the 2 methods are in good agreement (Table I), although the moment obtained by surface wave inversion gives a better fit to the surface wave amplitude data (Figure 2). In these two cases depth was fixed at the hypocentral value (5km) which provided a good fit to the body wave data. The depth from surface waves is less well constrained, but the variations of the mechanism (less than 5° on each plane) and moment (less than 30%) is within the uncertainty given by the comparison of the 3 independent solutions. Figure 4 shows a typical example of fit to the near field data for a small earthquake (M_W 2.9) in the vicinity of station MHC. The moment tensor solution, indicated by shading, is 95% double-couple.

Discussion and Conclusions

We are currently able to achieve a complete moment tensor catalogue down to M 4.5 with good confidence on the obtained solutions, using two and sometimes three independent methods, based on the analysis of regional surface waves, body waves and near-field data. With the accumulation of careful path calibrations in the surface wave and body wave methods, both for velocity and attenuation, this limit can be brought down to 4.0 in the near future, and the accuracy of the moment and depth estimates can be improved. However, we do not expect any significant changes to the results presented in Table I. The near-field analysis provides a means to estimate moment tensors in a robust fashion down to M 2 or less in the vicinity of any broadband stations, and this is now possible in several critical areas of central California (Bay Area, Parkfield). While data from dense short period arrays will remain crucial for the estimation of source parameters of earthquakes of M<3 in areas not instrumented by broadband stations, for the larger earthquakes, a sparse network of broadband stations yields more robust and accurate estimates of size and mechanism in a timely fashion.

We have illustrated here how the pattern of strain and stress release can be monitored continuously at the regional level, and its evolution with time systematically documented. For 1992-93, the observed patterns are entirely consistent with the previously determined state of stress in the region.

Acknowledgements. One of us (D.D.) wishes to thank C. Saikia for making available to him the FK integration code.

References

Bolt, B.A., J.E. Friday and R.A. Uhrhammer, A PC-based broadband digital seismograph network, Geophys. J. R. astr. Soc., 93, 565-573, 1988.

Dreger, D. S. and D. V. Helmberger, Determination of source parameters at regional distances with Single Station or Sparse Network Data, J. Geophys. Res., 98, 8107-8125, 1993.

Dziewonski, A.M., G. Ekstrom, J. Woodhouse and G. Zwart (1988) Centroid-moment tensor solutions for January-March, 1987, Phys.Earth Planet. Int., 50, 116-126.

Ekstrom, G., A system for automatic earthquake analysis, EOS, Trans. A.G.U., 73, 70, 1992

Kanamori, H., and E. Hauksson, TERRAscope, IRIS Newsletter, X, No. 2, 1-3, 1991.

Kanamori, H., and J. Given, Use of long-period surface waves for rapid determination of earthquake source parameters, Phys. Earth Planet. Inter., 27, 8-31, 1981.

Kanamori, H., J. Mori and T.H. Heaton, The 3 December 1988, Pasadena earthquake (ML=4.9) recorded with the very broadband system in Pasadena, Bull. Seism. Soc. Am., 80, 483-487, 1990.

Oppenheimer, D., G. Beroza, et al., The Cape Mendocino, California sequence of April 1992: subduction at the Triple Junction, Science, in press, 1993.

Patton, H., Reference point equilization method for determining the source and path effects of surface waves, J. Geophys. Res., 85, 821-848, 1980.

Patton, H., and G. Zandt, Seismic moment tensors of Western U.S. earthquakes and implications for the tectonic stress field, J. Geophys. Res., 96, 18245-59, 1991.

Romanowicz, B., Moment tensor inversion of long period Rayleigh waves: a new approach, J. Geophys. Res., 87, 5395-5407, 1982.

Romanowicz, B., and T. Monfret, Source process times and depths of large earthquakes by moment tensor inversion of mantle wave data and the effect of lateral heterogeneity, Annales Geoph., 74, 271-283, 1986.

Romanowicz, B., G. Anderson, L. Gee, R. McKenzie, D. Neuhauser., M.Pasyanos, and R. Uhrhammer, Real-time seismology at U.C. Berkeley, EOS Trans A.G.U., 73, 69, 1992.

Thio, H.K., and H. Kanamori, A surface wave study on the structure of the crust and upper mantle under Southern California, EOS Trans. A.G.U., 72, 324, 1991.

Uhrhammer, R., Broadband near-field moment tensor inversion , EOS Trans A.G.U., 73, 1992.

Zoback, M.L. and M.D.Zoback, State of stress in the conterminous United States, J. Geophys. Res., 85, 6113-6156, 1980.

Zoback, M., et al., New evidence on the state of stress of the San Andreas Fault System, Science, 238, 1105-1111, 1987.

B. Romanowicz, D. Dreger, M. Pasyanos and R. Uhrhammer, Seismographic Station, University of California, Berkeley, CA 94720.

(Received February 22, 1993;
revised May 14, 1993;
accepted June 8, 1993.)